Cancer Research

CRISPR/Cas9-Mediated Knockout of DGK Improves Antitumor Activities of Human T Cells

In-Young Jung, Yoon-Young Kim, Ho-Sung Yu, Myoungsoo Lee, Seokjoong Kim, and Jungmin Lee

Abstract

The efficacy of T-cell therapy is inhibited by various tumor-associated immunosuppressive ligands and soluble factors. Such inhibitory signals turn specific T-cell signaling pathways on or off, impeding the anticancer functions of T cells. Many studies have focused on PD-1 or CTLA-4 blockade to invigorate T-cell functions through CD28/B7 signaling, but obtaining robust clinical outcomes remains challenging. In this study, we use CRISPR/Cas9 to potentiate T-cell function by increasing CD3 signaling via knockout of diacylglycerol kinase (DGK), an enzyme that metabolizes diacylglycerol to phosphatidic acid. Knockout of DGK augmented the effector functions of CAR-T cells *in vitro* via increased TCR signaling. DGK knockout from CAR-T cells rendered them resistant to soluble immunosuppressive factors such as TGFβ and prostaglandin E2 and sustained effector functions under conditions of repeated tumor stimulation. Moreover, DGK knockout caused significant regression of U87MGvIII glioblastoma tumors through enhanced effector functions in a xenograft mouse model. Collectively, our study shows that knockout of DGK effectively enhances the effector functions of CAR-T cells, suggesting that CRISPR/Cas9-mediated knockout of DGK could be applicable as part of a multifaceted clinical strategy to treat solid cancers.

Significance: This novel study demonstrates efficient ablation of diacylglycerol kinase in human CAR-T cells that leads to improved antitumor immunity and may have significant impact in human cancer immunotherapy. *Cancer Res; 78(16); 4692–703. ©2018 AACR.*

Introduction

Chimeric antigen receptor (CAR) T cells have emerged as the leading paradigm for treating various hematologic malignancies. Treatment with CD19-targeting CAR-T cells resulted in complete remission (CR) rates of 82% to 94% and 50% to 75% for B-cell acute lymphoblastic leukemia (ALL) and chronic lymphoblastic leukemia (CLL), respectively (1). However, despite this success in blood cancers, CAR-T therapy has not shown efficient antitumor activity against solid cancers, such as lung, colon, breast, and brain cancers, except for a promising clinical outcome of anti-GD2 CAR-T cells against neuroblastoma (2). This failure can be attributed to multiple barriers posed by established solid tumors. The first hurdle is a mismatch between the chemokine receptors on T cells and the chemokines secreted by tumors, which significantly hampers efficient T-cell trafficking to the tumor site (3). Furthermore, even if CAR-T cells reach inside the tumors, their anticancer activities can be compromised by multiple layers of immunosuppressive mechanisms induced by a range of checkpoint inhibitors and soluble factors (e.g., PD-1, LAG-3, TIM-3, TGFβ, prostaglandin E2 (PGE2), and indoleamine-2,3-dioxygenase, etc.; refs. 4–6). Lastly, although CAR-T cells effectively control tumors, the loss of target antigen in tumors can lead to outgrowth of tumor antigen escape variants as observed in CD19 and CD22 CAR-T therapies, because CAR-T cells target only specific antigen (7, 8).

To overcome the immunosuppressive tumor microenvironment (TME), the CD28/B7 pathway, signal2, has been intensively targeted by programmed cell death protein 1 (PD-1) or cytotoxic T lymphocyte-associated antigen 4 (CTLA-4) blockade. PD-1 signal inhibition with anti-PD-1 antibody treatment or PD-1 knockout (KO) by TALEN or CRISPR/Cas9 has been carried out to potentiate T-cell effector functions (9–11). However, in many clinical trials, only some patients with cancer benefited from PD-1 blockade because patients with low PD-L1 expression in tumor and TME are less responsive to PD-1 blockade (12). Also, although T cells successfully circumvent immunosuppressive effect of the PD-1/PD-L1 pathway, other factors in TME, such as TIM-3, TGFβ, PGE2, and adenosine, provide a multidimensional immunosuppressive mechanism (4–6). Among those, TGFβ, PGE2, and adenosine directly or indirectly inhibit T-cell receptor (TCR) signaling, signal1, which is distinct from PD-1-mediated signal2 suppression (13, 14). Thus, engineering T cells to circumvent multiple signal1 inhibitory factors may yield a new strategy for promising therapeutic effects in immunosuppressive solid tumors.

Diacylglycerol kinase (DGK) is an enzyme that phosphorylates diacylglycerol (15) to phosphatidic acid (PA). Because DAG interacts with essential proteins involved in CD3 signaling such as protein kinase C (PKC) and Ras activating protein (RasGRP1),

ToolGen, Inc., Seoul, Korea.

Note: Supplementary data for this article are available at Cancer Research Online (http://cancerres.aacrjournals.org/).

I.-Y. Jung, Y.-Y. Kim, and H.-S. Yu contributed equally to this article.

Corresponding Author: Jungmin Lee, ToolGen, #1204, Byucksan Digital Valley 6-cha, 219 Gasan Digital 1-ro, Seoul, Seoul 08501, South Korea. Phone: 82-2-873-8168; E-mail: jm.lee@toolgen.com

doi: 10.1158/0008-5472.CAN-18-0030

activation of DGK results in downregulation of TCR distal molecules, including extracellular signal-related kinases 1/2 (ERK1/2; ref. 16). Two DGK isotypes, DGKα and DGKζ, are dominantly expressed in T cells. Although the two DGK isotypes share the common function of DAG metabolism, they are not fully redundant because their expression and activation are regulated in a disparate manner. In recent years, many studies have revealed the DGKα to be a potential inhibitory immune checkpoint, because they are specifically upregulated in tumor-infiltrating anergic T cells in human patients with renal cell cancer and xenograft mouse models (17–19). Also, inhibition of DGKα by small molecules reinvigorated the effector function of hypofunctional tumor-infiltrating immune cells (18). Based on these previous studies, it is strongly hypothesized that inhibition of DGK in human T cells may have strong therapeutic potential for cancer immunotherapy (17–19).

Despite wide recognition of immunosuppressive function of DGK in T cells (20), there exist overarching caveats regarding our understanding of DGK from previous studies when considering clinical applications of DGK inhibition for T cell therapy. For example, it is uncertain which isoform predominantly controls the antitumor effect between DGKα and DGKζ (21, 22). Also, T-cell response of DGKαζ KO cells in bacterial infection and tumor model is contradictory. Although DGKαζ KO enhanced effector function against mesothelioma (23), it significantly impaired the T-cell response against *Listeria monocytogenes* (24). Moreover, DGK KO in the mouse alters inflammatory functions of other immune cells such as dendritic cells and macrophages, which may affect T-cell biology (25, 26). In addition to these issues, immunologic differences between human and mouse T cells exist. For instance, unlike mouse T cells, human CD8 T cells lose CD28 expression during the developmental process (27). This is critical because CD28 inhibits DGKα activity and DGKα-mediated anergy. Thus, considering the disparate costimulatory signals and dysfunction mechanisms between the two species, as well as the promising therapeutic potential of DKG inhibition, studies in human T cells are imperative for clinical applications of DGK inhibition. However, existing methods for DGK inhibition in human T cells are challenging. DGKα inhibitors such as R59022 and R59949 lack specificity, inhibiting a broad range of DGK isotypes. Furthermore, there are no DGKζ inhibitors available to date (28).

Here, we sought to characterize the effects of knocking out DGKα (αKO) and DGKζ (ζKO) in human primary T cells by specifically disrupting the DGK isotypes using CRISPR/Cas9. Because compensatory immunosuppressive responses and T-cell anergy in the TME limit the efficacy of CAR-T cells in the clinic, we hypothesized that engineered CAR-T cells resistant to an inhospitable TME could result in enhanced efficacy against cold tumors, such as glioblastoma (29). We found that disruption of DGKα and DGKζ synergistically potentiates the effector function and proliferation of CAR-T cells by activating ERK signaling. Also, DGKαζ KO (dKO) CAR-T cells were less sensitive to T-cell hypofunction induced by tumor cell rechallenge and soluble immunosuppressive factors, such as TGFβ and PGE2. Moreover, dKO CAR-T cells significantly enhanced antitumor effect in a tumor xenograft mouse model, compared with control and DGK single KO CAR-T cells. Collectively, our data indicate that targeting DGK using CRISPR/Cas9 is a promising approach for cancer immunotherapies.

Materials and Methods

Tumor cell lines and media

The EGFRvIII-positive U87 MG glioblastoma cell line (U87vIII) was purchased from Celther Polska. The A375P melanoma cell line was obtained from the Korean Cell Line Bank. Cells were cultured in DMEM supplemented with 10% fetal bovine serum (FBS) and penicillin/streptomycin. *Mycoplasma* contamination was regularly monitored in all cell lines used in this study using the BioMycoX Mycoplasma PCR Detection Kit (CellSafe).

Lentivirus production

The 139 CAR, a fusion protein that contains an anti-EGFRvIII ScFV fused with a CD8 hinge, 4-1BB, and a CD3ζ domain, and a c259 TCR construct targeting NY-ESO-1 have been previously described (30, 31). The codon optimized sequences of the CAR and TCR constructs were subcloned into the lentiviral pLVX vector (Clontech). Viruses were collected from the supernatants of 293T cells transfected with the lentivirus vector and helper plasmids using Lipofectamine2000 (Thermo Scientific). After harvesting the supernatant, the lentivirus was overlaid on a 20% sucrose-containing buffer [100 mmol/L NaCl, 0.5 mmol/L ethylenediaminetetraacetic acid (EDTA), 50 mmol/L Tris-HCl, pH 7.4] at a 4:1 ratio and centrifuged at 10,000 × *g* at 4°C for 4 hours. Following centrifugation, the supernatant was removed, and phosphate-buffered saline (PBS) was added for resuspension.

Construction of DGK KO 139 CAR-T cells

CRSPR/Cas9-mediated genome editing of T cells was carried out as described with modifications. Human peripheral blood pan-T cells were purchased from STEMCELL Technologies. Upon thawing, the T cells were rested overnight in RPMI supplemented with FBS, hrIL2 (Peprotech, 50 U/mL) and hrIL7 (Peprotech, 5 ng/mL) prior to activation. Activation was induced by adding Dynabeads Human T Activator anti-CD3/28 (Thermo Scientific) at bead-to-cell ratio of 3:1 in RPMI supplemented with 10% FBS. After 24 hours of activation, T cells were replated on cell culture dishes coated with Retronectin (100 μg/mL) and the 139 CAR lentivirus for 48 hours. Three days after activation, activating beads were removed and electroporation was carried out using an Amaxa P3 Primary Cell kit and 4D-Nucleofecter (Lonza). Forty micrograms of recombinant *S. pyogenes* Cas9 (ToolGen) and 10 μg of chemically synthesized tracr/crRNA (Integrated DNA Technologies) were incubated for 20 minutes prior to electroporation to generate Cas9-gRNA ribonucleoprotein (RNP) complexes. A total of 3×10^6 stimulated T cells resuspended in P3 buffer were added to the preincubated Cas9-gRNA RNP complexes. Cells were nucleofected using program EO-115. Following electroporation, cells were seeded at 5×10^5 cells/mL in RPMI supplemented with 10% FBS, hIL2 (Peprotech, 50 U/mL) and hIL7 (Peprotech, 5 ng/mL). The following crRNA targeting sequences were used in the study: AAVS1: 5′-CCATCGTAAGCAAACCTTAG-3′, DGKα: 5′-CTCTCAAGCTGAGTGGGTCC-3′, DGKζ: 5′-ACGAGCACTCACCAGCATCC-3′, PD-1: 5′- GTCTGGGCGGTGCTACAACT-3′.

Flow cytometry staining and antibodies used in this study

Cell staining was performed at 4°C in PBS supplemented with 1% FBS unless otherwise indicated. Antibodies and reagents used for flow cytometry and functional studies were

as follows: CellTrace CFSE/Far red (Thermo Scientific), 7-aminoactinomycin (7-AAD, Sigma), anti-CD3: UCHT1 (BD), anti-CD45RO: UCHL1 (BD), anti-CCR7: 150513 (BD), anti-PD-1: EH12.2H7 (Biolegend), anti-FAS: Dx2 (BD), anti-Ki67: B56 (BD), anti-LAG-3: T47-530 (BD), anti-T-bet: 4B10 (Biolegend), anti-IFNγ: B27 (BD), anti-TNFα: Mab11 (BD), anti-PD-L1: 29E.2A3 (Biolegend), anti-TIM-3: 7D3 (BD), anti-EGFRvIII: (Biorbyt), goat anti-human IgG: (BioRad). Data were collected on an Attune NxT Acoustic Focusing Cytometer (Thermo Scientific) and analyzed using FlowJo (FlowJo, LLC).

In vitro killing assay, cytokine release, and proliferation assay

A total of 2×10^4 to 5×10^4 cells from the U87vIII and A375P cancer cell lines prestained with CellTrace Far red (Invitrogen) were cocultured with their cognate 139 CAR-T cells or C259 T cells at the indicated effector:target (E:T) ratios. After 18 hours of coincubation, cells were harvested and stained with 7-AAD for live/dead cell discrimination. Samples were acquired on an Attune NxT Acoustic Focusing Cytometer (Thermo Scientific) and analyzed with FlowJo (FlowJo, LLC). Cytotoxicity was calculated as [(% lysis sample − % lysis minimum)/(% lysis max [100%] − % lysis minimum)] × 100%. Triplicate experiments were performed. The supernatant from the coculture was analyzed using an ELISA Kit (Biolegend) or LEGENDplex (Biolegend) to measure IL2, IFNγ, and TNFα release. For TGFβ and PGE2 resistance assay, 10 ng/mL of TGFβ (RND Systems) or 0.5 μg/mL of PGE2 (Abcam) were treated with T cells for 18 hours. For proliferation assays, 4 days after coincubation of CellTrace-labeled 139 CAR-T cells with U87vIII cells, the distribution of CellTrace in the 139 CAR-T cells was assessed using flow cytometry.

Tumor cell rechallenging experiment

For serial tumor stimulation experiment, 139 CAR-T cells were coincubated with U87vIII cells at a ratio of E:T = 1:1 in RPMI supplemented with FBS, on day 0. On day 4, 139 CAR-T cells were harvested and replated with new U87vIII cells at the same E:T ratio. Supernatants were collected 24 hours after the first and second tumor stimulations to assess IFNγ and IL2 release.

Western blot analysis

For Western blot assays, cells were harvested and lysed in RIPA lysis and extraction buffer (Thermo Scientific, 89901) containing proteinase inhibitors (Thermo Scientific, 78442). Generally, total protein lysates from 1×10^5 cells were separated in 10% to 12% acrylamide gel, transferred to nitrocellulose membrane, blocked with 5% skim milk in TBS, blotted with each primary and secondary antibody diluted in TBS, washed with 0.1% Tween 20-TBS, and detected with SuperSignal West Femto Maximum Sensitivity Substrate (Thermo Scientific). Chemiluminescent images were captured by Fusion Solo (Vilber Lourmat). Rabbit anti-DGKα (Abcam, ab64845), rabbit anti-DGKζ (Abcam, ab105195), rabbit anti-Actin (Sigma A2066), rabbit anti-phospho-ERK1/2 (Tyr202/Tyr204; Cell Signaling, 9101), rabbit anti-ERK1/2 (Cell Signaling, 9102), HRP-conjugated Goat Anti-Rabbit IgG (Millipore, AP132P) were used for this research.

Calcium influx

Calcium influx in T cells was analyzed using a calcium assay kit (BD) according to the manufacturer's instructions. Briefly, T cells were washed with RPMI medium, resuspended in the same medium, and incubated with loading dye for 1 hour at 37°C. After acquiring the basal level of FITC signal from nontreated cells, anti-CD3 activation beads (Miltenyi Biotec) were added at a bead-to-cell ratio of 5:1, and the FITC signal was measured by flow cytometry. The data collected from flow cytometry were analyzed by FlowJo software using the kinetic mode.

Real-time PCR

For qRT-PCR, total RNA was isolated from T cells 7 days after CRISPR/Cas9 delivery using RNeasy Mini kit (Qiagen) following the manufacturer's instruction. cDNA was reverse transcribed from these RNAs using High Capacity cDNA Reverse Transcription Kit (Thermo Scientific) and qRT-PCR was done with QuantStudio3 (Applied Biosystems) using Power SYBR Green PCR Master Mix (Thermo Scientific) or TaqMan gene expression assay kit/probe sets (Thermo Scientific). The primers used in this study were as follows: hDGKα F: 5′-AATACCTGGATTGGGATGTGTCT-3′, hDGKα R: 5′-GTCCGTCGTCCTTCAGAGTC-3′, hDGKζ F: 5′-GTACTGGCAACGACTTGGC-3′, hDGKζ R: 5′-GCCCAGGCTGAAGTAGTTGTT-3′, hβ-Actin F: 5′-GGCACTCTTCCAGCCTTC-3′, hβ-Actin R: 5′-TACAGGTCTTTGCGGATGTC-3′, ID2: Hs00747379_m1, PRDM1: Hs00153357_m1, IL10: Hs00174086_m1, IFNG: Hs00174143_m1, IL2: Hs00174114.

Digenome-sequencing

Digenome-sequencing, an unbiased method for profiling Cas9 off-target effects, was performed as previously described (32). Genomic DNA from human T cells was isolated using a DNeasy Tissue kit (Qiagen). Genomic DNA (20 μg) was mixed with Cas9 protein (10 μg), crRNA (3.8 μg), and tracrRNA (3.8 μg) in a 1,000 μL reaction volume (NEB 3.1 buffer), and incubated for 4 hours at 37°C. The *in vitro*–digested DNA was then incubated with RNase A (50 μg/mL) for 30 minutes at 37°C and purified with a DNeasy Tissue kit (Qiagen). Digested DNA was fragmented using the Covaris system and ligated with adaptors for library formation. DNA libraries were subjected to whole genome sequencing using an Illumina HiSeq X Ten Sequencer at THERAGEN ETEX. We used the Isaac aligner to generate a Bam file using the following parameters: ver. 01.14.03.12; human genome reference, hg19 from UCSC (original GRCh37 from NCBI, Feb. 2009); base quality cutoff: 15; keep duplicate reads: yes; variable read length support: yes; realign gaps: no; and adaptor clipping: yes (adaptor: 5′-AGATCGGAAGAGC-3′, 5′-GCTCTTCCGATCT-3′).

Mouse xenograft studies

All the mice used in this study were maintained in the specific pathogen-free facility of Genexine, Inc., and the experiments were conducted under the SOP and followed the guidelines of the animal ethics committee. All animal experiments were approved by the Genexine's Institutional Animal Care and Use Committee (study 17-09-12). The mouse xenograft studies are conducted as below with modifications. In the U87vIII tumor model, 6- to 8-week-old female NSG mice were injected subcutaneously with 1×10^6 U87vIII cells into the right flank, in a volume of 100 μL PBS, on day 0. 28 days after implantation, when tumor sizes reached 250 ± 100 mm^2, the mice were randomized and divided into groups. Each group consists of 6 to 8 mice and tumor sizes were similar among groups. For each group, 5×10^6 T cells were infused on day 28 and day 32. All mice received

daily intraperitoneal administration of temozolomide (TMZ; Sigma; 0.33 mg/mouse/day) on days 32 to 35. Surface CAR expression levels on AAVS1 KO 139 CAR-T cells and DGKαζ KO 139 CAR-T cells were identical. Tumor sizes were monitored with calipers twice a week, and tumor volumes were calculated using the formula $V = (L \times W^2)/2$, where V is the tumor volume, L is the tumor length, and W is the tumor width. The animals were sacrificed when the tumor diameter reached 2000 mm^3. For further investigation of CAR-T cells after *in vivo* delivery, peripheral blood, spleen, and tumor tissues were isolated from each mouse. To dissociate tumor tissue, tumor samples were minced with scissors and treated with collagenase IV (100 U/mL) and DNase I (20 U/mL) for 1 hour in 37°C water bath. Cells were then passed through a sterile cell strainer for further investigations. To isolate cells from spleen, tissue was crushed with sterile plungers and passed through strainers. For lysis of red blood cells, cell suspensions were further treated with ACK buffer (150 mmol/L NH_4Cl, 10 mmol/L $KHCO_3$, 1 mmol/L EDTA, pH 7.2) for 5 minutes. To analyze effector function of tumor-infiltrating T cells, cells dissociated from tumor tissue were reactivated with phorbol 12-myristate 13-acetate (PMA, 50 ng/mL) and ionomycin (1 μg/mL) in the presence of GolgiStop (BD) for 5 hours in a CO_2 incubator and intracellular staining of IFNγ and TNFα was conducted.

Immunohistochemistry

For immunohistochemistry, tumor samples were excised and placed in 4% paraformaldehyde at 4°C for overnight. After another overnight washing with tap water, samples went through serial dehydration, were embedded in paraffin, and then were cut at a thickness of 4 μm. Sections were deparaffinized in xylene, rehydrated in absolute and 90% ethanol serially, and washed with running distilled water. After antigen retrieval in citrate buffer (0.01 mol/L, pH 6.4), they were incubated in blocking solution (5% horse serum, 3% BSA, 0.1% Tween 20 in PBS) for 4 hours at room temperature and then incubated with mouse anti-human CD3 antibody (Biolegend, Clone: OKT3) at 4°C, for overnight in a humidified chamber. Sections were then washed 4 times with PBS, incubated 1 hour at room temperature with Alexa Fluor 594 goat anti-mouse IgG H&L antibody (Molecular probe, ab150116), and then washed with PBS several times. Hoechst 33342 (BD, 561908) was added to the sections, and after 3 times of washings, slides were mounted using Vectashield (Vector Laboratories, H-1000). Images were taken with a Zeiss Axio Imager A2 microscope and Diagnostic SPOTFlex camera. Images were analyzed using the ImageJ software.

Results

Efficient disruption of DGK by CRISPR/Cas9 in primary human T cells

We tested guide RNAs (gRNA), which targeted sequences in exons 5 to 7 in the case of DGKα (αKO) or exons 3 to 12 in the case of DGKζ (ζKO), by electroporating CRISPR/Cas9 RNP (ribonucleoprotein) complexes into Jurkat human T cells (Supplementary Fig. S1A and S1B). After optimization of CRISPR/Cas9 RNP delivery via electroporation and the lentiviral transduction process (Fig. 1A), CRISPR/Cas9-treated 139 CAR-T cells exhibited robust expression of the CAR (Fig. 1B), which is highly selective against EGFRvIII and is designed to target

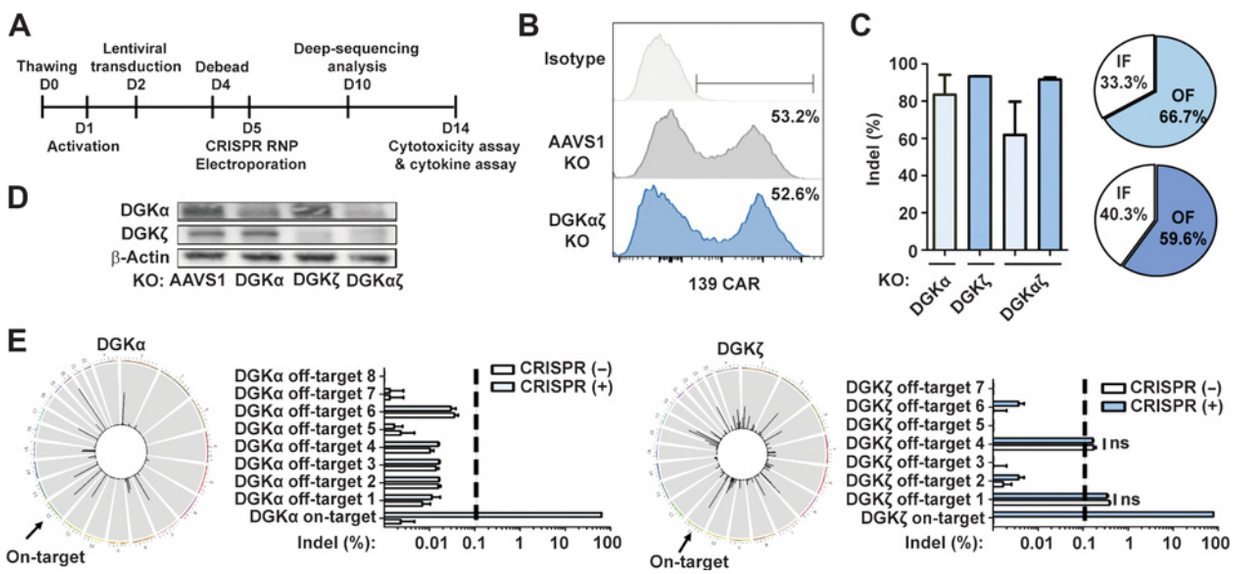

Figure 1.

Efficient DGK KO by CRISPR/Cas9 RNP delivery to primary human T cells. **A,** Schematic of the experimental strategy to express CAR in and to deliver CRISPR/Cas9 RNPs (ribonucleoproteins) to primary human T cells. **B,** Expression of 139 CAR was assessed by flow cytometry. **C,** KO efficiency was analyzed by targeted deep sequencing using the Mi-seq system (left). Representative out-of-frame rates were evaluated based on sequence analysis of DGKα and DGKζ KO cell populations (IF, in-frame; OF, out-of-frame, right). **D,** Representative Western blot analysis for DGK. **E,** Digenome-seq was used for unbiased analysis of off-target effects. Left, circos plots of genome-wide *in vitro* DNA cleavage scores. Arrows, on-target cleavage site. Right, Targeted deep sequencing aimed at potential off-target sites for which the cleavage score was higher than 10 (cutoff criteria: indel frequency < 0.1%). $N = 3$. Error bars, SEM; ns, not significant by Student t test. **B–D,** Experiments were done with T cells from three independent healthy donors.

glioblastoma cells as described elsewhere (31). The small insertion/deletion (indel) rate in the αKO and ζKO experiments ranged from 80% to 90% (Fig. 1C). A detailed sequence analysis at the cleavage sites revealed that the frequency of out-of-frame mutations induced by nonhomologous end joining (NHEJ) repair was 66.7% and 59.6% in αKO and ζKO 139 CAR-T cells, respectively, which corresponds to the reduction of the DGK mRNA and protein level (Fig. 1D; Supplementary Fig. S2A and S2B). Double and single KO showed comparable knockout efficiency in primary human T cells (Fig. 1C). The KO process did not significantly affect cell proliferation or viability (Supplementary Fig. S2C and S2D). To investigate off-target effects of DGK-targeting CRISPR/Cas9, we conducted mismatch-based *in silico* analysis and Digenome-seq., an unbiased genome-wide method for profiling off-target effects (32). Targeted deep sequencing of potential off-target sites identified by both *in silico* analysis and Digenome-seq. demonstrated no significant off-target effects in either αKO or ζKO 139 CAR-T cells (Fig. 1E; Supplementary Fig. S3A and S3B). Collectively, the results indicate that CRISPR/Cas9 allows efficient and isotype-specific DGK KO without affecting cell physiology and the level of CAR expression in primary human T cells.

DGK KO improves effector functions of 139 CAR-T by amplifying TCR distal signal.

Because enhanced cytokine secretion by ζKO mouse T cells was previously reported by other groups, we assessed the antitumor function of DGK KO 139 CAR-T cells (23, 33). In *in vitro* characterization studies, we used AAVS1 KO 139 CAR-T cells (AAVS1 139 CAR-T) as a negative control. Compared with the AAVS1 139 CAR-T cells, the DGK KO 139 CAR-T cells showed a superior effector function as demonstrated by significant increase in cytotoxicity and cytokine secretion after coincubation with U87vIII cells (the U87MG glioblastoma cell line expressing EGFRvIII; Fig. 2A and B). Expression levels of CAR indicate that the enhanced effector function of DGK KO 139 CAR-T cells does not attribute to CAR expression *per se* (Supplementary Fig. S4A). Moreover, DGK KO 139 CAR-T cells did not have nonspecific activity against U87MG, which does not express EGFRvIII, confirming specificity and safety of DGK KO 139 CAR-T (Supplementary Fig. S4B–S4D). Interestingly, dKO 139 CAR-T cells produced more IFNγ and IL2 than did αKO or ζKO 139 CAR-T cells, suggesting synergistic effect of dKO in antitumor activity. We also examined whether PD-1 blockade would further increase the effector function of DGK KO 139 CAR-T cells by using PD-L1–positive U87vIII cells (Supplementary Fig. S5A). Although both AAVS1 139 CAR-T cells and dKO 139 CAR-T cells expressed PD-1 after coincubation with U87vIII (Supplementary Fig. S5B), we observed no further increase in cytotoxicity or IFNγ secretion when cells were treated with anti-PD-1 antibody, except for αKO 139 CAR-T cells with only slight increase in IFNγ secretion (Fig. 2C and D). We next examined the activation of the TCR downstream signal in DGK KO cells. We stimulated AAVS1 and DGK KO 139 CAR-T cells with anti-CD3 beads for the indicated time and measured calcium influx and TCR distal signal, phospho-ERK (pERK; Fig. 2E and F). Although calcium influx was unaffected by DGK KO (Fig. 2F), ERK phosphorylation

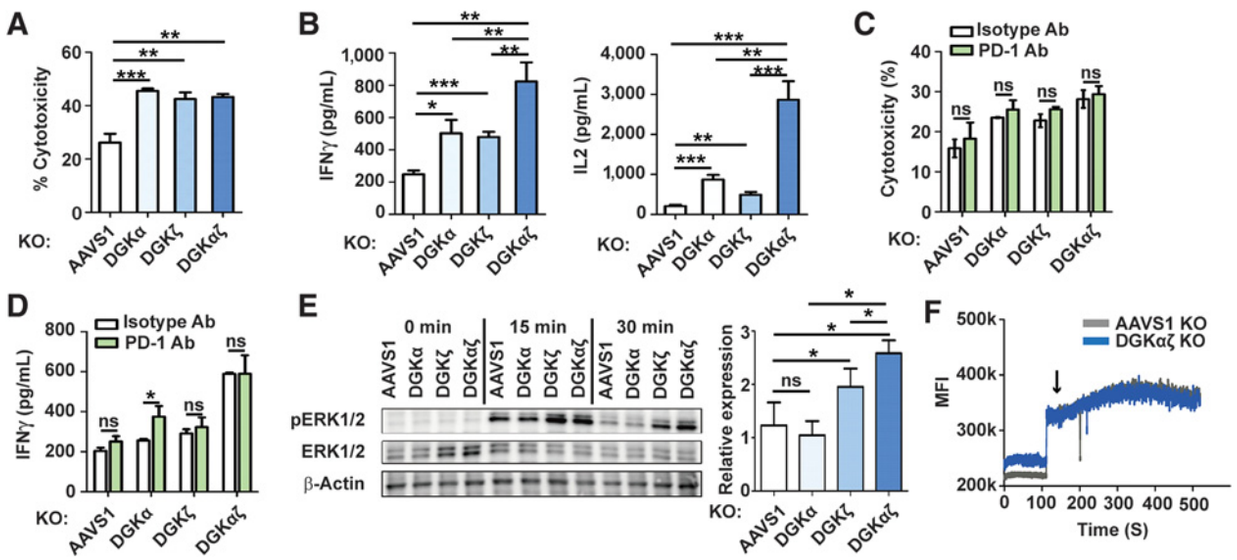

Figure 2.

DGK KO improves effector functions of 139 CAR-T by amplifying TCR distal signal. Engineered 139 CAR-T cells and CellTrace-treated U87vIII cells were incubated at a ratio of E:T = 1:2 in a 96-well plate for 20 hours. **A,** The killing activity of 139 CAR-T cells was assessed by measuring the percentage of 7-AAD–positive U87vIII cells using flow cytometry. **B,** IFNγ and IL2 release were analyzed by ELISA. **C** and **D,** The 139 CAR-T cells and U87vIII cells were incubated at a ratio of E:T = 1:2 for 20 hours with or without anti-PD-1 antibody (20 μg/mL). **C**, Killing activity. **D**, IFNγ release. **E,** T cells were stimulated with CD3/CD28 beads for the indicated time and assessed for phosphorylated ERK by Western blot. Left, representative Western blot; right, relative expression of pERK1/2 to ERK1/2. Experiments were conducted using T cells from three different healthy donors, and a representative Western blot result is presented. **F,** CD3-mediated calcium influx was determined by flow cytometry during activation of T cells with CD3 beads (arrow, time point of T-cell activation). $N = 3$. Error bars, SEM. *, $P < 0.05$; **, $P < 0.01$; ***, $P < 0.001$; ns, not significant by Student t test. **A–D**, Representative data of two independent experiments carried out in triplicate. MFI, mean flourescence intensity.

was amplified and lasted longer in ζKO and dKO T cells (Fig. 2E). A marked increase in phosphorylated ERK signaling in dKO T cells is consistent with the dKO synergistic effector function seen in Fig. 2B. These data indicate that DGK KO augments TCR distal signaling and thereby increases the effector functions of 139 CAR-T cells.

CRISPR/Cas9-mediated DGK KO CAR-T cells circumvent the immunosuppressive effects of TGFβ and PGE2 in 139 CAR-T cells

Based on the data showing that DGK KO effectively invigorated TCR distal signaling, we examined whether DGK KO could reduce the sensitivity of 139 CAR-T cells to signal1 inhibitors. Among different inhibitory factors, we focused on TGFβ and PGE2, because the therapeutic effects of CAR-T cells have been limited due to the elevated level of TGFβ and PGE2 in the immunosuppressive TME (13, 29, 34). First, we investigated the inhibitory effect of TGFβ on 139 CAR-T cell activity against U87vIII cells. AAVS1, αKO, and ζKO 139 CAR-T cells exposed to high physiologic concentrations of TGFβ (10 ng/mL) showed reduced IFNγ and IL2 production (Fig. 3A–D; Supplementary Fig. S6A–S6D). In contrast, dKO 139 CAR-T cells maintained their effector function upon TGFβ treatment. Likewise, dKO 139 CAR-T cells were relatively insensitive to the inhibitory factor PGE2 compared with AAVS1, αKO, and ζKO 139 CAR-T cells (Fig. 3E–H; Supplementary Fig. S6E–S6H). Normalization data showed that although AAVS1 139 CAR-T cells showed a remarkable loss of responsiveness to tumor cells, dKO 139 CAR-T cells exhibited sustained antitumor function, maintaining their effector function under the exposure to TGFβ and PGE2 (Fig. 3D and H; Supplementary Fig. S6D and S6H). The marginal decrease in the antitumor activity of dKO 139 CAR-T cells in the presence of TGFβ or PGE2 treatment might be a result of incomplete disruption of the DGK genes in the dKO, given that the out-of-frame rate in αKO and ζKO was 66.7% and 59.6%, respectively (Fig. 1C). These data indicate that the DGK double KO enabled 139 CAR-T cells to overcome immunosuppression of signal1 inhibitors. We also examined the beneficial role of the dKO in c259 TCR-T cells, selectively targeting NY-ESO-1. When cocultured with A375P cells expressing NY-ESO, effector function of dKO c259 TCR-T cells treated with TGFβ or PGE2 was comparable with that of AAVS1 KO c259 TCR-T without inhibitor treatment (Supplementary Fig. S6I–S6N). These data demonstrate the versatility of the dKO approach in adoptive cell transfer.

CRISPR/Cas9-mediated DGK KO renders T cells less hypofunctional during repeated tumor stimulation

Upon repetitive antigen recognition, T cells often exhibit loss of IL2 secretion and cytotoxicity and enter a hypofunctional state. DAG metabolism is a key determinant that regulates T-cell activation and anergy (35, 36). Because previous studies have reported that an anergic state in mouse T cells can be reversed by pharmacologic inhibition of DGKα, we investigated whether DGK KO would allow human T cells to overcome dysfunctional state (19, 36). First, we assessed the proliferative capacity of dKO 139 CAR-T cells upon tumor cell rechallenge. After AAVS1 and dKO 139 CAR-T cells were incubated with U87vIII cells for 96 hours, the 139 CAR-T cells were rechallenged with U87vIII cells and expansion of the 139 CAR-T

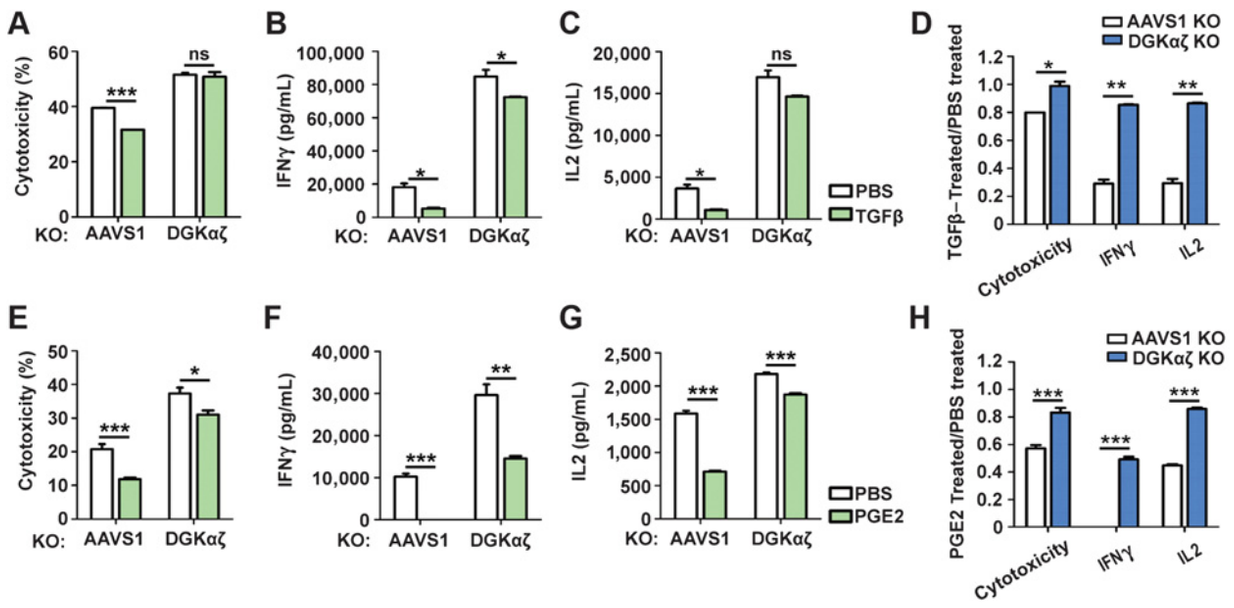

Figure 3.

CRISPR/Cas9-mediated DGK KO CAR-T cells circumvent the immunosuppressive effects of TGFβ and PGE2. The 139 CAR-T cells and CellTrace-treated U87vIII cells were incubated at a ratio of E:T = 3:1 for 18 hours. **A–C,** Killing activity (**A**), IFNγ secretion (**B**), and IL2 secretion (**C**) by 139 CAR-T cells were assessed in the presence or absence of TGFβ (10 ng/mL). **E–G,** Killing activity (**E**), IFNγ secretion (**F**), and IL2 secretion (**G**) by 139 CAR-T cells were assessed in the presence or absence of PGE2 (0.5 μg/mL). **D** and **H,** The fold changes in cytotoxicity, IFN γ secretion, and IL2 secretion are represented by TGFβ/PBS treated (**D**) and PGE2/PBS treated (**H**). $N = 3$. Error bars, SEM. *, $P < 0.05$; **, $P < 0.01$; ***, $P < 0.001$; ns, not significant by Student t test. Representative data of two independent experiments carried out in triplicate are shown.

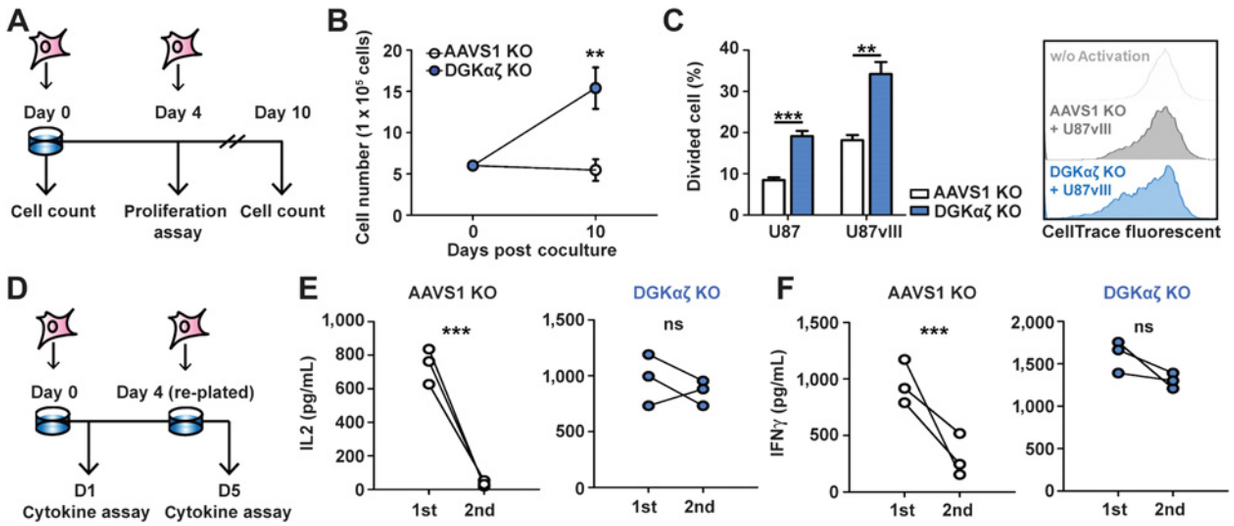

Figure 4.

CRISPR/Cas9-mediated DGK KO renders T cells less hypofunctional during repeated tumor stimulation. **A,** Schematic of tumor cell rechallenge experiment. CellTrace-labeled 139 CAR-T cells were incubated with tumor cells at a ratio of E:T = 3:1 on days 0 and day 4. **B,** T-cell proliferation between days 0 and 10. **C,** Frequency of dividing 139 CAR-T cells on day 4. Left, percentage of dividing cells in the presence of U87 or U87vIII tumor cells. Right, representative proliferation histogram. **D,** U87vIII cells were coincubated with 139 CAR-T cells at a ratio of E:T = 1:1 on day 0. On day 4, T cells were replated with U87vIII cells at the same E:T ratio. Supernatants were collected 24 hours after each tumor cell challenge to assess IL2 (**E**) and IFNγ (**F**). $N = 3$, Error bars, SEM. **, $P < 0.01$; ***, $P < 0.001$; ns, not significant by Student t test. Representative data of two independent experiments carried out in triplicate are shown.

cells was measured by CellTrace distribution and cell counting (Fig. 4A). In contrast to AAVS1, αKO, and ζKO 139 CAR-T cells that exhibited marginal proliferation, dKO 139 CAR-T cells successfully proliferated upon repeated tumor stimulation (Fig. 4B and C; Supplementary Fig. S7A and S7B). To determine whether the superior expansion of dKO 139 CAR-T cells is attributed to an enhanced proliferation or reduced AICD (activation induced cell death), we assayed for apoptotic cells using 7-AAD. When 139 CAR-T cells that had encountered U87vIII cells stained with 7-AAD, the frequency of 7-AAD–positive T cells was slightly higher in the dKO 139 CAR-T population than in the AAVS1 139 CAR-T population (Supplementary Fig. S7C). Because it was reported that inhibition of DGKα induces FAS-dependent apoptosis in T cells (37), we assessed FAS expression in T cells, which revealed that FAS surface expression was increased in dKO 139 CAR-T cells compared with AAVS1 139 CAR-T cells (Supplementary Fig. S7D). These data indicate that enhanced dKO 139 CAR-T cell growth upon repeated tumor stimulation is primarily due to increased cell proliferation, which offsets the slight increase in AICD, presumably mediated by FAS expression. We then analyzed levels of cytokine secretion from dKO 139 CAR-T cells after second tumor stimulation (Fig. 4D–F). Although AAVS1 139 CAR-T cells produced IFNγ and IL2 robustly on the first U87vIII stimulation, they showed a significant loss of cytokine secretion after the second U87vIII stimulation (Fig. 4E and F). In contrast, dKO 139 CAR-T cells sustained cytokine secretion in respond to the second U87vIII-mediated activation. We also examined whether cytokine level of dKO 139 CAR-T upon second tumor stimulation is attributed to sustained CAR expression, because antigen-induced CAR internalization can limit antitumor efficacy (38). However, we observed a similar level of reduction in CAR expression in both AAVS1 and dKO 139 CAR-T after antigen encounter (Supplementary Fig. S7E). These results indicate that dKO 139 CAR-T maintains effector function during repeated tumor stimulation by regulating anergic pathway not CAR expression.

CRISPR/Cas9-mediated DGK KO reprograms T cells toward the effector memory subset

Loss of both DGKα and DGKζ has been reported to skew mouse CD8 T-cell differentiation toward short-lived effector cells and an effector memory population. Because the composition of the memory T-cell population affects clinical outcomes (39), we examined whether DGK KO induces changes in 139 CAR-T cell subsets. We characterized dKO 139 CAR-T subsets after coincubating these cells with U87vIII cells for 4 days. Before the tumor stimulation, the dKO 139 CAR-T cells showed a smaller naïve T-cell population than did the AAVS1 139 CAR-T cells (Fig. 5A). After 4 days of tumor encounter, the naïve dKO 139 CAR-T cell population preferentially differentiated into effector memory cells, which resulted in smaller naïve and central memory T-cell populations (Fig. 5A and B). We next investigated whether dKO reprograms 139 CAR-T cells transcriptionally. After 2 days of T-cell activation using CD3/28 dynabeads, there was a dynamic increase in the expression of transcription factors that regulate effector memory cells, such as *ID2* and *PRDM1*, in DGKαζ T cells (Fig. 5C and D). Also, *IL10*, a type II cytokine, was significantly reduced in dKO 139 CAR-T cells (Fig. 5E), whereas levels of type I cytokines, such as *IFNγ* and *IL2*, were markedly elevated (Fig. 5F and G). Finally, we examined the exhaustion markers PD-1 and TIM-3 in dKO 139 CAR-T cells to ensure that the effector memory population induced by dKO is not dysfunctional. After activation of 139 CAR-T cells with U87vIII for 7 days, dKO and AAVS1 139

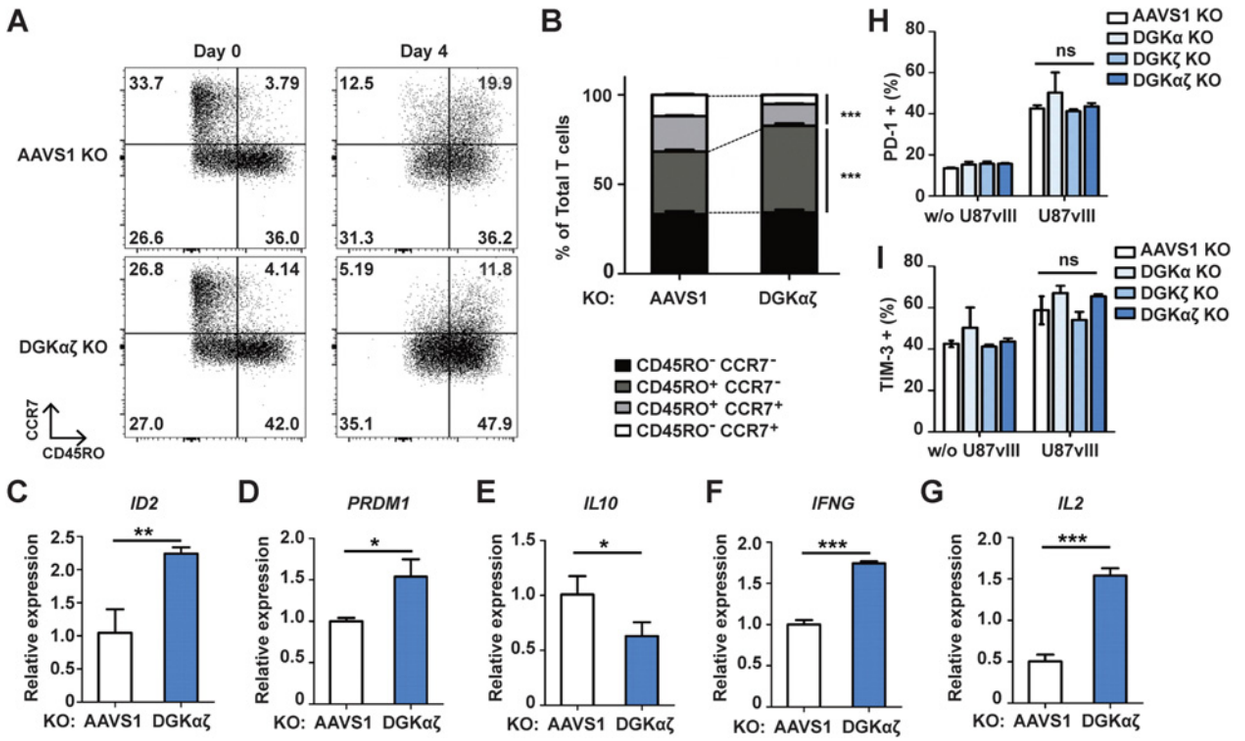

Figure 5.

DGK KO reprograms 139 CAR-T cells toward an effector memory phenotype. Subsets of 139 CAR-T and dKO 139 CAR-T cells were examined before and after coincubation with U87vIII cells. $CD45RO^{-}CCR7^{+}$, $T_{Naïve}$; $CD45RO^{+}CCR7^{+}$, T_{cm} (central memory T); $CD45RO^{+}CCR7^{-}$, T_{em} (effector memory T). **A,** Representative histograms of T-cell memory subsets before and after activation. **B,** Summary of T-cell subsets in populations of each KO variant. **C–G,** qRT-PCR analysis of AAVS1 139 CAR-T and dKO 139 CAR-T cells after activation using CD3/CD28 dynabeads to determine *ID2* (**C**), *PRDM1* (**D**), *IL10* (**E**), *IFNG* (**F**), and *IL2* (**G**) expression levels. Exhaustion markers PD-1 (**H**) and TIM-3 (**I**) were analyzed in 139 CAR-T cells 7 days after activation with U87vIII cells. $N = 3$, Error bars, SEM. *, $P < 0.05$; **, $P < 0.01$; ***, $P < 0.001$; ns, not significant by the Student t test.

CAR-T cells showed a similar level of PD-1 and TIM-3 expression (Fig. 5H and I). Based on these results, we conclude that KO of DGK transcriptionally reprograms 139 CAR-T cells toward an effector memory phenotype without exacerbating exhaustion, which results in robust antitumor effects *in vitro*.

CRISPR/Cas9-mediated DGK KO improves tumor clearance by enhancing *in vivo* effector function.

To optimize injection route of 139 CAR-T cells and investigate antitumor effect of DGK KO *in vivo*, we transferred T cells, AAVS1 139 CAR-T cells, and dKO 139 CAR-T cells into U87vIII-implanted NSG mice, intravenously (i.v.; Fig. 6A) or intratumorally (i.t.; Fig. 6B), respectively. Because the effectiveness of adoptive cell transfer can vary dramatically depending on the tumor burden and the number of immune cells that are injected, we adopted a "high tumor burden with low T-cell dose" model to clearly distinguish the *in vivo* efficacy of dKO 139 CAR-T cells from that of the control AAVS1 139 CAR-T cells (9). We injected the first dose of 139 CAR-T cells 28 days after tumor injection when the tumor volume reached 250 ± 100 mm^3, and the second dose of 139 CAR-T cells 4 days after the first 139 CAR-T injection. The approximate E:T ratios of the first and second injections were 1:10 and 1:20, respectively. The adjuvant TMZ was administered daily from the day of second 139 CAR-T cell infusion for 4 days to promote tumor regression as previous studies have shown that anti-EGFRvIII CAR-T cell therapy is often ineffective without TMZ (40, 41). All i.v. injection groups showed tumor growth retardation after TMZ treatment after day 32; however, AAVS1 139 CAR-T cells failed to control tumor regression (Fig. 6A and C). In contrast, dKO 139 CAR-T cells caused significant tumor regression on day 56 in tumor xenograft mice and showed increased number of tumor-infiltrating T cells (Fig. 6A, C–E). Tumor growth profile and number of tumor-infiltrating T cells in i.t. injection setting were consistent with those of the i.v. injection experiment, showing that i.v. injected 139 CAR-T cells can effectively traffic to tumor microenvironment and exert their antitumor effect (Fig. 6B–E).

To further characterize the *in vivo* function of DGK KO 139 CAR-T cells, we i.v. injected AAVS1, αKO, ζKO, and dKO 139 CAR-T cells as described above and analyzed effector function and proliferative capacity of those cells. Although we again confirmed that dKO 139 CAR-T cells showed superior tumor control and tumor infiltration, αKO and ζKO 139 CAR-T cells failed to improve antitumor effect *in vivo* (Fig. 6F and G). We also found that ζKO and dKO 139 CAR-T cells significantly increased polyfunctional tumor-infiltrating T cells that secrete cytokines and show enhanced T-cell proliferation (Fig. 6H and I). Interestingly, we observed that both tumor-infiltrating and circulating dKO 139 CAR-T cells highly expressed multiple inhibitory immune checkpoints such as PD-1, TIM-3, and LAG-3, which can be either T-cell exhaustion or activation

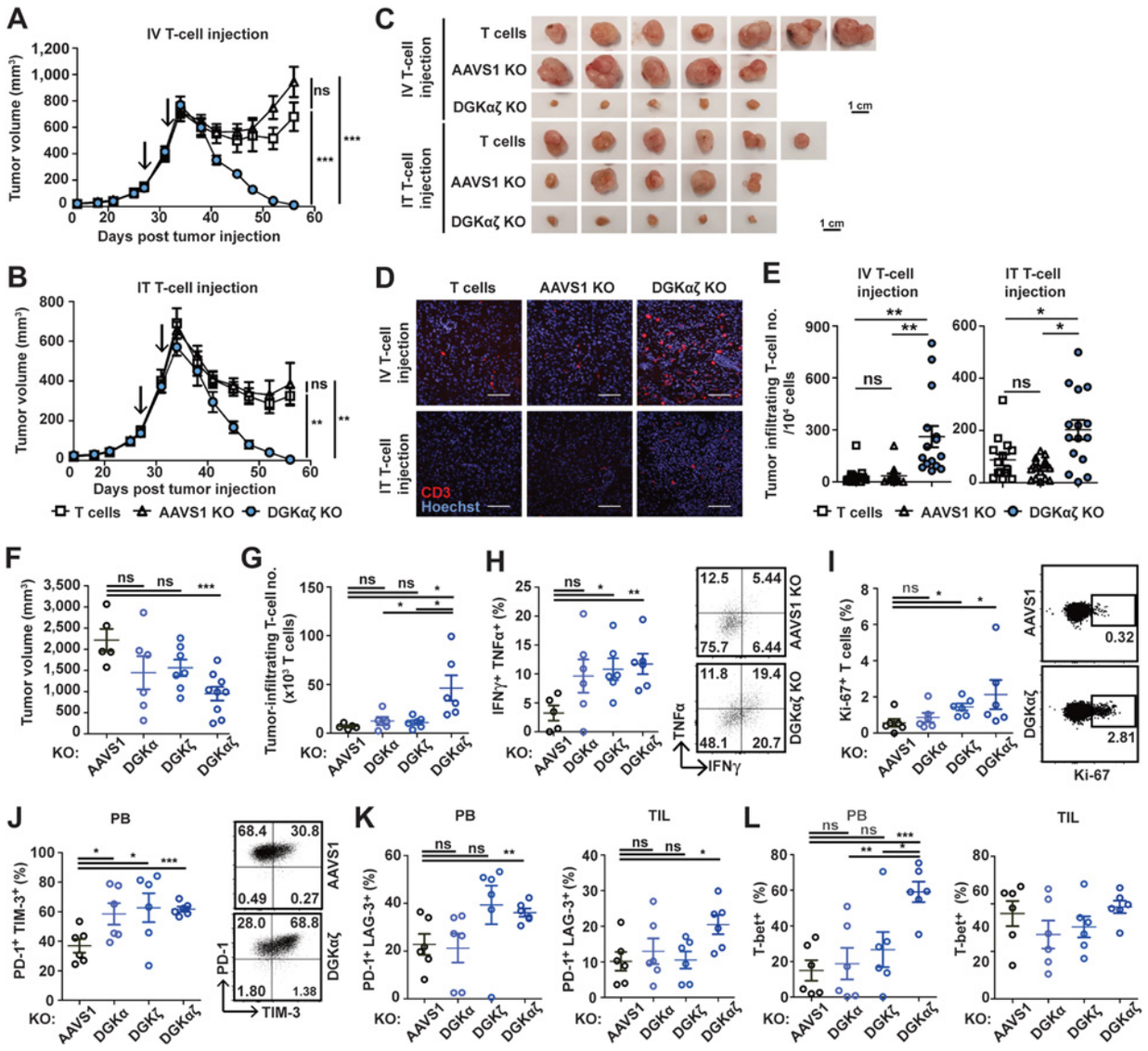

Figure 6.

CRISPR/Cas9-mediated DGK KO improves tumor clearance by enhancing *in vivo* effector function. **A–E,** NSG mice were injected with 1×10^6 U87vIII cells subcutaneously. On days 28 and 32, 5×10^6 T cells, AAVS1 139 CAR-T cells, and dKO 139 CAR-T cells were infused i.v. (**A**) or i.t. (**B**) All mice received daily intraperitoneal administration of TMZ (0.33 mg/mouse/day) during days 32 to 35. Tumor regression induced by dKO 139 CAR-T cells was observed after i.v. injection (**A**) and i.t. injection (**B**; $n = 6$–8 for each i.v. and i.t. experiment). The values and error bars represent mean tumor size ($mm^3 \pm$ SEM). **C,** Microscopic images of tumors. Scale bars, 1 cm. **D,** Infiltrating T cells were visualized by immunohistochemistry using anti-human CD3 antibody. CD3, red; Hoechst, blue. Scale bars, 300 μm. **E,** Infiltrating human T cells were calculated from captured images by following formula. Infiltrating T-cell number in 10^4 cells = [(CD3$^+$ T cells)/(Hoechst$^+$ cells)] × 10,000. **F–L,** NSG mice were injected with 1×10^6 U87vIII cells subcutaneously, and then AAVS1, αKO, ζKO, and dKO 139 CAR-T cells along with TMZ were injected as described above. **F,** Tumor volume at day 55 after U87vIII injection ($n = 5$–7). **G,** Number of tumor-infiltrating CD3$^+$ human T cells ($n = 5$–7). **H,** IFNγ and TNFα expression in tumor-infiltrating CD3$^+$ human T cells after reactivation for 5 hours ($n = 5$–7). **I,** Ki-67 expression in circulating CD3$^+$ human T cells ($n = 5$–7). **J,** PD-1 and TIM-3 expression in circulating CD3$^+$ human T cells ($n = 6$–7). **K,** PD-1 and LAG-3 expression in circulating and tumor-infiltrating CD3$^+$ human T cells ($n = 6$–7). **L,** T-bet expression in circulating and tumor-infiltrating CD3$^+$ human T cells ($n = 6$–7). PB, peripheral blood; TIL, tumor-infiltrating lymphocytes. *, $P < 0.05$; **, $P < 0.01$; ***, $P < 0.001$; ns, not significant by the Student *t* test.

markers (Fig. 6J and K). Of note, dKO 139 CAR-T cells express much more T-bet in peripheral blood compared with other groups, suggesting they sustain more effector function (Fig. 6L). Given that dKO 139 CAR-T cells are largely T-bet positive with enhanced effector function and proliferation capacity, it is suggested that the increased multiple inhibitory immune checkpoints are markers for functional effector T cells, not exhausted T cells (Fig. 6H, I, and L).

Because dKO 139 CAR-T cells highly upregulated PD-1 in tumor-infiltrating population, we knocked out endogenous

PD-1 of 139 CAR-T cells to further enhance antitumor efficacy as conducted by previous studies (9–11, 42). Using optimized knockout process, we achieved more than 75% of indel in PD-1 target locus in 139 CAR-T cells, *in vitro* (Supplementary Fig. S8A). We then injected 139 CAR-T cells 22 days after tumor infusion without coadministrating TMZ, and isolated T cells 20 days after T-cell injection to analyze PD-1 expression. Consistent with our previous *in vivo* experiments, dKO 139 CAR-T cells highly upregulated PD-1 (Supplementary Fig. S8B) and PD-1 KO 139 CAR-T cells and PD-1/DGKαζ KO 139 CAR-T cells successfully suppressed PD-1 expression (Supplementary Fig. S8B). Interestingly, contrary to the previous studies that have reported beneficial effect of PD-1 inhibition, PD-1 KO 139 CAR-T cells failed to improve antitumor effect, while dKO 139 CAR-T cells successfully enhanced tumor control and effector function in our xenograft mouse model (Supplementary Fig. S8C and S8D). Likewise, PD-1 disruption in dKO 139CAR-T cell did not further increase antitumor effect (Supplementary Fig. S8C and S8D).

Collectively, our results indicate that knocking out both DGKα and DGKζ using CRISPR/Cas9 synergistically improves *in vivo* antitumor efficacy where inhibition of PD-1 fails to invigorate antitumor effect of CAR-T cells.

Discussion

The CRISPR/Cas9 system has enabled manipulation of immune checkpoint inhibitors in T cells to enhance the antitumor activity (9). However, considering the multiple layers of immunosuppression in the inhospitable TME and current pitfalls associated with T-cell therapy in the clinic, there is a strong need to find new targets to manipulate to increase the effectiveness of such approaches.

Downregulation of DGK in T cells could be a promising strategy for immunotherapy because DGK is specifically upregulated in nonresponsive tumor-infiltrating lymphocytes and is a master regulator of T-cell hypofunction (35, 36, 43). However, despite its therapeutic potential for improving T-cell activity in cancer, current trials to downregulate DGK are highly limited by the following restrictions. First, because DGKs are intracellular molecules, they are not suitable antibody targets. Second, there are not yet any specific inhibitors of DGKα or DGKζ. For example, the most commonly used DGKα inhibitors, R59949 and R59022, broadly attenuate other DGK isotypes, such as DGKε, DGKθ, DGKγ, DGKκ, and DGKδ (28). Thus, clinical application of such inhibitors would probably be associated with undesirable effects; it is known that mutations in some of the isotypes, such as DGKθ and DGKδ, cause neuronal defects (44, 45). Lastly, systemic administration of DGK inhibitors would also pose significant safety concerns, given that systematic deficiency of DGKα and DGKζ has been shown to significantly impair T-cell development in mice and that DGKζ has been suggested to protect hippocampal neurons from ischemia (46, 47). For these reasons, deploying CRISPR/Cas9 could be a compelling technology, providing a safe and precise method to knock out specific DGK isotypes without causing significant off-target effects (Fig. 1E; Supplementary Fig. S3A and S3B). Additionally, *ex vivo* engineering of T cells does not alter DGK activity in other tissues in the body. Moreover, our approach of using CRISPR/Cas9 can be used combinatorially to knock out multiple genes simultaneously. For instance, because dKO 139 CAR-T cells have been shown to exhibit increased apoptosis-inducing FAS expression (Supplementary Fig. S7D), the combination of FAS KO with DGK dKO would be a promising engineering approach to further increase the efficacy of CAR-T cells in the clinic.

In this study, we demonstrate highly effective CRISPR/Cas9-mediated gene editing without a need for selection to enrich the DGK KO cells. Because 5′-triphosphate group in guide RNA induces type I interferon responses, causing cell death and low editing efficiency, we deployed modified guide RNA in our RNP (ribonucleoprotein) electroporation process, and thereby achieved high rate of gene editing (80%–90%) in human primary T cells with minimum cell growth inhibition (Fig. 1; Supplementary Fig. S2; refs. 48, 49). Also to minimize off-target mutation, we screened guide RNA with minimum mismatch sequence in genome, and used RNP complex for rapid turnover of Cas9 in cells (50). These optimized gene-editing process resulted in highly effective gene editing in human primary T cells with no significant off-target effect (Fig. 1; Supplementary Fig. S3).

In this study, we revealed that disruption of DGK potentiates the antitumor function of human CAR-T cells as previously described by others in mouse CAR-T cells (23, 33). We and others have shown that αKO and ζKO enhanced effector functions to a similar extent (Figs. 2 and 6; refs. 23, 33). These data contradict the predominant role of DGKζ in amplifying TCR downstream signal, pERK, after strong stimulation with CD3 antibody (Fig. 2E; refs. 18, 51). This is probably due to the difference in regulatory mechanisms between DGKα and DGKζ. Whereas DGKα plays a predominant role in weak TCR signaling, which leads to T-cell anergy, DGKζ is an inhibitor of Ras–ERK signaling in response to strong TCR signals. Thus, the difference in strength of CD3 signaling between strong CD3 antibody-mediated stimulation *in vitro* and CAR-mediated stimulation *in vivo* may result in the contradictory result (52). In addition, we observed the synergistic effect of DGK dKO compared with single KO variants, which also coincides with the observations of Riese and colleagues (23). Because these data suggest the nonredundant role of DGKα and DGKζ, disrupting both isotypes would be crucial for fully invigorating T-cell antitumor activity.

Recently, many studies have aimed at making T cells resistant to certain inhibitory checkpoints, such as PD-1 or LAG-3 (9, 51). Although such manipulations successfully circumvent the inhibitory effects of specific ligands, such as PD-L1 and MHC class II, these engineered T cells acquired resistance only to their corresponding inhibitory pathway. Instead of targeting individual TGFβ or PGE2 receptors, we targeted a key intracellular protein, DGK, to increase the availability of DAG, which is depleted by various signal1 inhibitors in the TME. We found that dKO 139 CAR-T cells acquired resistance against signal1 inhibitors (Fig. 3). The results strongly suggest that our CRISPR/Cas9-based DGK KO approach would be an efficient way to boost the efficacy of CAR-T cell therapy, especially in the presence of immune inhibitors in the TME. Further investigation is needed to examine the resistance of DGK KO CAR-T cells to other immunosuppressive molecules such as adenosine and LAG-3.

Though our study illustrates a successful gene engineering strategy to improve the efficacy of T-cell therapy, our approach may raise safety concerns. CAR-T cell therapy often induces life-threatening cytokine release syndrome and neurotoxicity, which is one of the most crucial barriers in the clinic. In this respect, the

increased cytokine production and cytotoxicity of dKO 139 CAR-T cells would pose significant safety issues. There have been several recent approaches to tackle this safety problem. Sen and colleagues showed that targeting the exhaustion-specific enhancer of PD-1 by CRISPR/Cas9 allows specific downregulation of PD-1 in exhausted T cells, alleviating safety concerns of constitutive PD-1 knockout (53). Shum and colleagues demonstrated a successful application of safety switch, an inducible caspase9, to their engineered T cells, which resulted in 93% clearance of the infused T cells after administration of a chemical inducer in a mouse model (54). In addition, KO of the TCR in CAR-T cells can mitigate the potential risks of autoimmunity induced by autoreactive T cell clones. It would be worth adapting these strategies to address the safety issues associated with our DGK KO 139 CAR-T cells and to render them more tunable.

Interestingly, we observed no enhancement of antitumor efficacy in the PD-1 inhibition group in both our *in vitro* and *in vivo* setting where U87vIII and T cells highly expressed PD-L1 and PD-1, respectively (Fig. 2C and D; Supplementary Fig. S8). In contrast to PD-1 KO, DGK KO approach successfully enhanced antitumor efficacy in our mouse model, possibly by increasing effector function and resistance to signal1-targeting inhibitors, such as TGFβ, which is highly upregulated in glioblastoma TME (29). Also, DGK KO enhances antitumor efficacy irrelevant to PD-L1 or B7 ligands expression. This implies promising therapeutic potential of the DGK KO approach in glioblastoma, where PD-1 blockade failed to provide survival benefit in patients (55).

Here, we identified DGK as a potential TCR checkpoint molecule, and specifically knocked out DGK using CRISPR/Cas9 technology. Our engineering approach demonstrates the crucial role of DGK in activating CD3 signaling to invigorate the antitumor effects of T-cell therapy, an approach that is distinct from previous studies that primarily focused on reactivation of the CD28 pathway through PD-1 blockade. Our study highlights therapeutic implications of DGK that could be applied to enhance clinical outcomes of T-cell therapy for solid tumors.

Disclosure of Potential Conflicts of Interest

I.-Y. Jung, Y.-Y. Kim, H.-S. Yu, M. Lee, S. Kim, and J. Lee have ownership interest (including stock, patents, etc.) in an entity.

Authors' Contributions

Conception and design: I.-Y. Jung, Y.-Y. Kim, S. Kim, J. Lee
Development of methodology: H.-S. Yu, M. Lee
Acquisition of data (provided animals, acquired and managed patients, provided facilities, etc.): I.-Y. Jung, Y.-Y. Kim, H.-S. Yu, M. Lee
Analysis and interpretation of data (e.g., statistical analysis, biostatistics, computational analysis): I.-Y. Jung, Y.-Y. Kim, H.-S. Yu, M. Lee, J. Lee
Writing, review, and/or revision of the manuscript: I.-Y. Jung, Y.-Y. Kim, M. Lee, J. Lee
Study supervision: Y.-Y. Kim, S. Kim, J. Lee

Acknowledgments

This work was supported by the National Research Foundation of Korea (NRF-2018M3A9H3020844 and NRF-2017M3A9B4061406).

The costs of publication of this article were defrayed in part by the payment of page charges. This article must therefore be hereby marked *advertisement* in accordance with 18 U.S.C. Section 1734 solely to indicate this fact.

Received January 3, 2018; revised April 29, 2018; accepted June 19, 2018; published first July 2, 2018.

References

1. Park JH, Geyer MB, Brentjens RJ. CD19-targeted CAR T-cell therapeutics for hematologic malignancies: interpreting clinical outcomes to date. Blood 2016;127:3312–20.
2. Louis CU, Savoldo B, Dotti G, Pule M, Yvon E, Myers GD, et al. Antitumor activity and long-term fate of chimeric antigen receptor-positive T cells in patients with neuroblastoma. Blood 2011;118:6050–6.
3. Slaney CY, Kershaw MH, Darcy PK. Trafficking of T cells into tumors. Cancer Res 2014;74:7168–74.
4. Koyama S, Akbay EA, Li YY, Herter-Sprie GS, Buczkowski KA, Richards WG, et al. Adaptive resistance to therapeutic PD-1 blockade is associated with upregulation of alternative immune checkpoints. Nat Commun 2016;7:10501.
5. Schietinger A, Philip M, Krisnawan VE, Chiu EY, Delrow JJ, Basom RS, et al. Tumor-specific T cell dysfunction is a dynamic antigen-driven differentiation program initiated early during tumorigenesis. Immunity 2016;45:389–401.
6. Chen JH, Perry CJ, Tsui YC, Staron MM, Parish IA, Dominguez CX, et al. Prostaglandin E2 and programmed cell death 1 signaling coordinately impair CTL function and survival during chronic viral infection. Nat Med 2015;21:327–34.
7. Fry TJ, Shah NN, Orentas RJ, Stetler-Stevenson M, Yuan CM, Ramakrishna S, et al. CD22-targeted CAR T cells induce remission in B-ALL that is naive or resistant to CD19-targeted CAR immunotherapy. Nat Med 2018;24:20–8.
8. Sotillo E, Barrett DM, Black KL, Bagashev A, Oldridge D, Wu G, et al. Convergence of acquired mutations and alternative splicing of CD19 enables resistance to CART-19 immunotherapy. Cancer Discov 2015;5:1282–95.
9. Rupp LJ, Schumann K, Roybal KT, Gate RE, Ye CJ, Lim WA, et al. CRISPR/Cas9-mediated PD-1 disruption enhances anti-tumor efficacy of human chimeric antigen receptor T cells. Sci Rep 2017;7:737.
10. Hui E, Cheung J, Zhu J, Su X, Taylor MJ, Wallweber HA, et al. T cell costimulatory receptor CD28 is a primary target for PD-1-mediated inhibition. Science 2017;355:1428–33.
11. Menger L, Sledzinska A, Bergerhoff K, Vargas FA, Smith J, Poirot L, et al. TALEN-mediated inactivation of PD-1 in tumor-reactive lymphocytes promotes intratumoral T-cell persistence and rejection of established tumors. Cancer Res 2016;76:2087–93.
12. Taube JM, Klein A, Brahmer JR, Xu H, Pan X, Kim JH, et al. Association of PD-1, PD-1 ligands, and other features of the tumor immune microenvironment with response to anti-PD-1 therapy. Clin Cancer Res 2014;20:5064–74.
13. Arumugam V, Bluemn T, Wesley E, Schmidt AM, Kambayashi T, Malarkannan S, et al. TCR signaling intensity controls CD8+ T cell responsiveness to TGF-beta. J Leukoc Biol 2015;98:703–12.
14. Wehbi VL, Tasken K. Molecular mechanisms for cAMP-mediated immunoregulation in T cells - Role of anchored protein kinase a signaling units. Front Immunol 2016;7:222.
15. Ma Q, Gonzalo-Daganzo RM, Junghans RP. Genetically engineered T cells as adoptive immunotherapy of cancer. Cancer Chemother Biol Response Modif 2002;20:315–41.
16. Riese MJ, Moon EK, Johnson BD, Albelda SM. Diacylglycerol kinases (DGKs): novel targets for improving T cell activity in cancer. Front Cell Dev Biol 2016;4:108.
17. Prinz PU, Mendler AN, Brech D, Masouris I, Oberneder R, Noessner E. NK-cell dysfunction in human renal carcinoma reveals diacylglycerol

kinase as key regulator and target for therapeutic intervention. Int J Cancer 2014;135:1832–41.
18. Prinz PU, Mendler AN, Masouris I, Durner L, Oberneder R, Noessner E. High DGK-alpha and disabled MAPK pathways cause dysfunction of human tumor-infiltrating CD8+ T cells that is reversible by pharmacologic intervention. J Immunol 2012;188:5990–6000.
19. Moon EK, Wang LC, Dolfi DV, Wilson CB, Ranganathan R, Sun J, et al. Multifactorial T-cell hypofunction that is reversible can limit the efficacy of chimeric antigen receptor-transduced human T cells in solid tumors. Clin Cancer Res 2014;20:4262–73.
20. Zhong X-P, Hainey EA, Olenchock BA, Jordan MS, Maltzman JS, Nichols KE, et al. Enhanced T cell responses due to diacylglycerol kinase ζ deficiency. Nat Immunol 2003;4:882.
21. Andrada E, Liebana R, Merida I. Diacylglycerol kinase zeta limits cytokine-dependent expansion of CD8+ T cells with broad antitumor capacity. EBioMedicine 2017;19:39–48.
22. Joshi RP, Schmidt AM, Das J, Pytel D, Riese MJ, Lester M, et al. The zeta isoform of diacylglycerol kinase plays a predominant role in regulatory T cell development and TCR-mediated ras signaling. Sci Signal 2013;6:ra102.
23. Riese MJ, Wang LC, Moon EK, Joshi RP, Ranganathan A, June CH, et al. Enhanced effector responses in activated CD8+ T cells deficient in diacylglycerol kinases. Cancer Res 2013;73:3566–77.
24. Yang J, Zhang P, Krishna S, Wang J, Lin X, Huang H, et al. Unexpected positive control of NFkappaB and miR-155 by DGKalpha and zeta ensures effector and memory CD8+ T cell differentiation. Oncotarget 2016;7:33744–64.
25. Singh BK, Kambayashi T. The immunomodulatory functions of diacylglycerol kinase zeta. Front Cell Dev Biol 2016;4:96.
26. Liu C-H, Machado FS, Guo R, Nichols KE, Burks AW, Aliberti JC, et al. Diacylglycerol kinase ζ regulates microbial recognition and host resistance to Toxoplasma gondii. J Exp Med 2007;204:781–92.
27. Noessner E. DGK-alpha: a checkpoint in cancer-mediated immuno-inhibition and target for immunotherapy. Front Cell Dev Biol 2017;5:16.
28. Sato M, Liu K, Sasaki S, Kunii N, Sakai H, Mizuno H, et al. Evaluations of the selectivities of the diacylglycerol kinase inhibitors R59022 and R59949 among diacylglycerol kinase isozymes using a new non-radioactive assay method. Pharmacology 2013;92:99–107.
29. O'Rourke DM, Nasrallah MP, Desai A, Melenhorst JJ, Mansfield K, Morrissette JJD, et al. A single dose of peripherally infused EGFRvIII-directed CAR T cells mediates antigen loss and induces adaptive resistance in patients with recurrent glioblastoma. Sci Transl Med 2017;9. pii: eaaa0984.
30. Rapoport AP, Stadtmauer EA, Binder-Scholl GK, Goloubeva O, Vogl DT, Lacey SF, et al. NY-ESO-1-specific TCR-engineered T cells mediate sustained antigen-specific antitumor effects in myeloma. Nat Med 2015;21:914–21.
31. Sampson JH, Choi BD, Sanchez-Perez L, Suryadevara CM, Snyder DJ, Flores CT, et al. EGFRvIII mCAR-modified T-cell therapy cures mice with established intracerebral glioma and generates host immunity against tumor-antigen loss. Clin Cancer Res 2014;20:972–84.
32. Kim D, Bae S, Park J, Kim E, Kim S, Yu HR, et al. Digenome-seq: genome-wide profiling of CRISPR-Cas9 off-target effects in human cells. Nat Methods 2015;12:237–43, 1 p following 43.
33. Shin J, O'Brien TF, Grayson JM, Zhong XP. Differential regulation of primary and memory CD8 T cell immune responses by diacylglycerol kinases. J Immunol 2012;188:2111–7.
34. Perng P, Lim M. Immunosuppressive mechanisms of malignant gliomas: parallels at non-CNS sites. Front Oncol 2015;5:153.
35. Zha Y, Marks R, Ho AW, Peterson AC, Janardhan S, Brown I, et al. T cell anergy is reversed by active Ras and is regulated by diacylglycerol kinase-alpha. Nat Immunol 2006;7:1166–73.
36. Olenchock BA, Guo R, Carpenter JH, Jordan M, Topham MK, Koretzky GA, et al. Disruption of diacylglycerol metabolism impairs the induction of T cell anergy. Nat Immunol 2006;7:1174–81.
37. Alonso R, Rodriguez MC, Pindado J, Merino E, Merida I, Izquierdo M. Diacylglycerol kinase alpha regulates the secretion of lethal exosomes bearing Fas ligand during activation-induced cell death of T lymphocytes. J Biol Chem 2005;280:28439–50.
38. Walker AJ, Majzner RG, Zhang L, Wanhainen K, Long AH, Nguyen SM, et al. Tumor antigen and receptor densities regulate efficacy of a chimeric antigen receptor targeting anaplastic lymphoma kinase. Mol Ther 2017;25:2189–201.
39. Gattinoni L, Lugli E, Ji Y, Pos Z, Paulos CM, Quigley MF, et al. A human memory T cell subset with stem cell-like properties. Nat Med 2011;17:1290–7.
40. Ohno M, Ohkuri T, Kosaka A, Tanahashi K, June CH, Natsume A, et al. Expression of miR-17-92 enhances anti-tumor activity of T-cells transduced with the anti-EGFRvIII chimeric antigen receptor in mice bearing human GBM xenografts. J Immunother Cancer 2013;1:21.
41. Johnson LA, Scholler J, Ohkuri T, Kosaka A, Patel PR, McGettigan SE, et al. Rational development and characterization of humanized anti-EGFR variant III chimeric antigen receptor T cells for glioblastoma. Sci Transl Med 2015;7:275ra22.
42. Su S, Hu B, Shao J, Shen B, Du J, Du Y, et al. CRISPR-Cas9 mediated efficient PD-1 disruption on human primary T cells from cancer patients. Sci Rep 2016;6:20070.
43. Baldanzi G, Pighini A, Bettio V, Rainero E, Traini S, Chianale F, et al. SAP-mediated inhibition of diacylglycerol kinase alpha regulates TCR-induced diacylglycerol signaling. J Immunol 2011;187:5941–51.
44. Tu-Sekine B, Raben DM. Regulation of DGK-theta. J Cell Physiol 2009;220:548–52.
45. Leach NT, Sun Y, Michaud S, Zheng Y, Ligon KL, Ligon AH, et al. Disruption of diacylglycerol kinase delta (DGKD) associated with seizures in humans and mice. Am J Hum Genet 2007;80:792–9.
46. Guo R, Wan CK, Carpenter JH, Mousallem T, Boustany RM, Kuan CT, et al. Synergistic control of T cell development and tumor suppression by diacylglycerol kinase alpha and zeta. Proc Natl Acad Sci U S A 2008;105:11909–14.
47. Ali H, Nakano T, Saino-Saito S, Hozumi Y, Katagiri Y, Kamii H, et al. Selective translocation of diacylglycerol kinase zeta in hippocampal neurons under transient forebrain ischemia. Neurosci Lett 2004;372:190–5.
48. Kim S, Koo T, Jee HG, Cho HY, Lee G, Lim DG, et al. CRISPR RNAs trigger innate immune responses in human cells. Genome Res 2018;28:367–73.
49. Hendel A, Bak RO, Clark JT, Kennedy AB, Ryan DE, Roy S, et al. Chemically modified guide RNAs enhance CRISPR-Cas genome editing in human primary cells. Nat Biotechnol 2015;33:985–9.
50. Kim S, Kim D, Cho SW, Kim J, Kim JS. Highly efficient RNA-guided genome editing in human cells via delivery of purified Cas9 ribonucleoproteins. Genome Res 2014;24:1012–9.
51. Zhang Y, Zhang X, Cheng C, Mu W, Liu X, Li N, et al. CRISPR-Cas9 mediated LAG-3 disruption in CAR-T cells. Front Med 2017;11:554–62.
52. Merida I, Andrada E, Gharbi SI, Avila-Flores A. Redundant and specialized roles for diacylglycerol kinases alpha and zeta in the control of T cell functions. Sci Signal 2015;8:re6.
53. Sen DR, Kaminski J, Barnitz RA, Kurachi M, Gerdemann U, Yates KB, et al. The epigenetic landscape of T cell exhaustion. Science 2016;354:1165–9.
54. Shum T, Omer B, Tashiro H, Kruse RL, Wagner DL, Parikh K, et al. Constitutive signaling from an engineered IL7 receptor promotes durable tumor elimination by tumor-redirected T cells. Cancer Discov 2017;7:1238–47.
55. Filley AC, Henriquez M, Dey M. Recurrent glioma clinical trial, CheckMate-143: the game is not over yet. Oncotarget 2017;8:91779–94.